Path Loss From a Transmitter Inside an Aircraft Cabin to an Exterior Fuselage-Mounted Antenna

Kathy Wei Hurst and Steven W. Ellingson, *Senior Member, IEEE*

***Abstract*—The increasing use of mobile electronic devices by passengers and equipment on large aircraft may increase the likelihood of interference with the aircraft's electronic systems. Thus, the "interference path loss" from a transmitting device inside the cabin of such aircraft to the antenna terminals of a victim system of the aircraft is of interest. Full-wave modeling and other deterministic techniques are impractical or undesirable for this purpose due to the potentially large electrical dimensions of the aircraft, as well as the variability of the cabin configuration. An alternative hybrid analysis technique applicable to frequencies above very high frequency is proposed in which one first estimates the power that escapes the cabin using a simple method based on microwave cavity theory. Next, the radiating windows are modeled as magnetic currents on a cylinder modeling the fuselage, and the resulting electric field at the location of the victim antenna is determined using the uniform geometrical theory of diffraction. Finally, the power delivered to the victim antenna is estimated as the coherent sum of fields incident from the windows. This technique yields results consistent with measured results and yields additional physical insight that would be difficult to obtain through measurements or full-wave methods.**

***Index Terms*—Aircraft antennas, indoor propagation, uniform geometrical theory of diffraction (UTD).**

I. Introduction

MODERN aircraft use a complex suite of electronic systems for navigation and communications [1]. Flight safety depends on the unimpeded operation of these systems. However, the increasing proliferation of mobile electronic devices such as cellular phones, wireless LAN-enabled computing devices, and radio-frequency identification (RFID) systems may increase the likelihood of interference. Thus, it is of interest to determine the path loss from a transmitting device inside the cabin of a transport aircraft to the RF input of a potential victim system of the aircraft. Given this "interference path loss" (IPL) and an estimate of the power radiated by the transmitter, the power delivered to a victim system can be determined and compared to known thresholds for vulnerability [2], [3] to determine the margin of safety. Previous efforts to measure IPL directly have demonstrated that accurate and repeatable measurements are difficult to obtain, yielding instead typically large variances with sensitive dependence on the measurement techniques employed [4]–[8]. Recently, an evolved measurement methodology for small aircraft has been reported [9]. An example of IPL analysis demonstrating the deleterious impact of IPL uncertainty is presented in [10]. A method for estimating IPL for cabin-to-antenna problems with accuracy comparable to direct measurements is desirable as a means to validate measurements, as a tool for interference vulnerability analysis generally, and for design and assessment of mitigation techniques.

This paper specifically considers the problem of how to determine IPL defined as the power delivered to the terminals of a victim antenna mounted on the fuselage, relative to the total power radiated by a transmitting device inside the cabin. A rigorous solution to this problem using full-wave integral equation methods is awkward due to the dimensions of the fuselage (tens of meters) relative to the wavelengths of interest, which can be as small as 60 mm, corresponding to the approximately 5-GHz frequency of operation of the microwave landing system (MLS). (However, it is noted that such analysis is quite practical for small vehicles at low frequencies; see, e.g., [11].) Furthermore, the configuration of the cabin is difficult to anticipate and can vary over time, and includes a complex collection of objects including people, seats, luggage, bulkheads, and cargo. Prior investigations (including those cited in the previous paragraph) have mostly bypassed this problem by focussing on the portion of the path loss measured from the point at which power leaves the fuselage, to the victim antenna. However, lossy materials within the cabin play a role in determining cabin-to-antenna IPL. Therefore, it is desirable that any new analysis technique yields reasonable estimates of IPL in the presence of these features, but at the same time should not require detailed information about the specific geometries or constitutive parameters of the media.

Thus, a more specific restatement of the problem addressed here is as follows. Consider a modern transport aircraft that includes a large cabin area. The cabin could be passenger space (i.e., seating), cargo space, or some combination of the two. An emitter transmits from an unspecified location in the cabin. The radiated signal propagates within the cabin, where it is either absorbed by the material in the cabin (such as seats or people), or escapes from the cabin through windows or possibly other mechanisms. Some fraction of the signal power that escapes from the cabin radiates away safely from the aircraft, whereas some remaining fraction will propagate along the surface of the fuselage and can be received by the victim antenna located somewhere along the dorsal (i.e., top or zenith facing) area of the fuselage. It is the IPL associated with this combination of mechanisms that is the focus of this paper.

The proposed solution to this problem consists of three steps. In the first step, the power that escapes the cabin through

Manuscript received November 28, 2007; revised April 16, 2008.

K. W. Hurst was with the Bradley Department of Electrical and Computer Engineering, Virginia Polytechnic Institute and State University, Blacksburg, VA 24061 USA. She is now with the United States Patent and Trademark Office, Alexandria, VA 22312 USA.

S. W. Ellingson is with the Bradley Department of Electrical and Computer Engineering, Virginia Polytechnic Institute and State University, Blacksburg, VA 24061 USA (e-mail: ellingson@vt.edu).

Color versions of one or more of the figures in this paper are available online at http://ieeexplore.ieee.org.

Digital Object Identifier 10.1109/TEMC.2008.926880

windows is estimated. Transmission through windows is assumed to be the dominant mechanism for power escape from the cabin, as opposed to other mechanisms such as leakage through gaps around doors, or conducted emission via wires. Evidence indicating that transmission through windows is in fact the dominant mechanism for escape from an aircraft cabin at frequencies above very high frequency (VHF) appears in [12]. (At VHF and lower frequencies, propagation along wiring and through door seams become important and should not be neglected.) In the second step, the radiating windows are treated as magnetic currents on a perfectly conducting cylinder modeling the fuselage exterior, and determine the resulting electric field at the location of the victim antenna. Finally, the power delivered to the victim antenna from the incident electric field is estimated using a simple model for the antenna. Because the phases of the equivalent magnetic current sources used in the second step are expected to be effectively randomly distributed, steps 2 and 3 are repeated many times in Monte Carlo fashion, varying the phases from trial to trial, to determine the distribution of possible IPLs. A finding from simulations for various aircraft is that the mean IPL determined using this procedure is typically about 20 dB greater than the minimum IPL.

The first step—estimating power that escapes the cabin through windows—is performed using a strategy referred to as "power balance theory" (PBT). PBT models the cabin as a cavity that contains only simple loss mechanisms, such as absorption in lossy materials and radiation through apertures, using the method of Hill *et al.* [13]. The results are independent of the geometry of the cavity and the position of the emitter, depending instead only on simple, general parameters such as the cavity volume, effective cross section of transmission (for windows), and effective cross section of absorption (for lossy materials). This is ideal in the present problem as it is not convenient to specify the position of the emitter nor the details of the geometry inside the cabin, for the obvious reasons that both can change and a more generally applicable characterization is desired. The PBT methodology is described further in Section II-A.

The second step involves calculation of the electric fields that propagate from windows to the victim antenna along the surface of the fuselage using a convex surface diffraction formulation of the uniform geometrical theory of diffraction (UTD) developed by Pathak and Wang [14]. The efficacy of UTD for predicting the propagation over the fuselage of large aircraft for frequencies as low as the VHF band was previously demonstrated in [15], although in that work, the application was to determine coupling between antennas. The UTD approach yields the desired results with very low computational effort and is described further in Section II-B.

Section II-C provides a complete, integrated description of the procedure for calculating IPL. This procedure is demonstrated by example in Section III, where it is applied to the study of IPL from the cabin to the global positioning system (GPS) antenna for various aircraft at the 1575 MHz "L1" frequency of operation. Section IV addresses the applicability of the method to other frequencies. Finally, conclusions are presented in Section V.

II. Theory

A. Calculating Power Escape Through Windows

PBT accounts for the dissipation of power radiated by a source in a cavity using the concept of *quality factor* Q, which can be interpreted as the ratio of energy dissipation over time to the total available power, where f is the frequency of interest. In the present problem, the cabin is treated as a microwave cavity having an overall quality factor given by

$$Q = \frac{2\pi f U_s}{P_d} \tag{1}$$

where U_s is the steady-state energy stored in the cabin and P_d is the total power dissipated. The cabin Q can also be determined from quality factors associated with various mechanisms that account for P_d as follows:

$$\frac{1}{Q} = \frac{1}{Q_1} + \frac{1}{Q_2} + \frac{1}{Q_3} + \frac{1}{Q_4} \tag{2}$$

where Q_1, Q_2, Q_3, and Q_4 are associated with losses due to wall conductivity, absorption in lossy materials, escape through apertures, and power captured by other antennas in the cabin, respectively. In the present problem, Q_2 accounts for power dissipation within seats, people, and other lossy objects; whereas Q_3 accounts for power escape through windows in the cabin. In each case

$$Q_n = \frac{2\pi f U_s}{P_{dn}}, \qquad \text{where } n = 1, 2, 3, 4 \tag{3}$$

and where P_{d1}, P_{d2}, P_{d3}, and P_{d4} are the power dissipation associated with Q_1, Q_2, Q_3, and Q_4, respectively. In order to satisfy the principle of conservation of power, P_d must be equal to the total power transmit P_T. Thus, the total power lost though windows relative to the total power transmitted is

$$L_w = \frac{P_{d3}}{P_T} = \frac{P_{d3}}{P_d}. \tag{4}$$

If it is assumed that the walls of the cabin have sufficiently high conductivity, and also no other antennas in the cabin with significant power-capturing ability are at the same frequency, then Q_1 and Q_4 will be large relative to Q_2 and Q_3. At frequencies above VHF, other sources of loss including coupling onto wiring and propagation through door seems are assumed to be negligible. In this case, one finds from (2) and (4) that

$$L_w \approx \frac{Q_2}{Q_2 + Q_3}. \tag{5}$$

Expressions for Q_2 and Q_3 are available from [13] as follows:

$$Q_2 = \frac{2\pi V}{\lambda \langle \sigma_a \rangle} \tag{6}$$

$$Q_3 = \frac{4\pi V}{\lambda \langle \sigma_t \rangle} \tag{7}$$

where V is the volume of the cavity, λ is free-space wavelength, $\langle \sigma_a \rangle$ is the mean absorption cross section for all lossy material in the cavity, and $\langle \sigma_t \rangle$ is the mean transmission cross section for all apertures in the cavity. In both cases, the mean is taken

over all possible angles of incidence; each being considered to be equally probable.

Reasonable estimates of $\langle \sigma_a \rangle$ are required. It is assumed that the sum of lossy material is accounted for by the combination of people and seats, and that all other material in the cabin has negligible loss in comparison. It is known from previous theoretical and experimental work on the effect of people on propagation in enclosed spaces that it is reasonable to model scattering and absorption statistically and/or using simple geometric models, and that the results are only weakly frequency dependent [16], [17]. It is also known from previous experimental work that the mean absorption cross section of a typical person $\langle \sigma_{ap} \rangle$ is about 0.4 m^2 at 2.4 GHz, and varies very slowly with frequency [18]. The absorption cross section of a typical seat $\langle \sigma_{as} \rangle$ is known to be approximately 0.04 m^2 at microwave frequencies, again varying very slowly with frequency [19]. Thus, one can estimate

$$\langle \sigma_a \rangle \approx N_p \langle \sigma_{ap} \rangle + N_s \langle \sigma_{as} \rangle \tag{8}$$

where N_p and N_s are the number of people and seats, respectively, in the cabin.

Reasonable estimates of $\langle \sigma_t \rangle$ are also required. As discussed in Section I, it is assumed that the dominant mechanism here is transmission through windows. It is further assumed that only the area—and not the shape—of windows is important, such that the windows can be modeled as circular apertures of radius a_w. From [13], one finds that the transmission cross section for a single window is

$$\langle \sigma_{tw} \rangle \approx \frac{\pi a_w^2}{2}, \qquad \text{if } ka_w > 1.29 \tag{9}$$

$$\langle \sigma_{tw} \rangle \approx \frac{16}{9\pi} k^4 a_w^6, \qquad \text{if } ka_w < 1.29 \tag{10}$$

with the former and latter expressions corresponding to windows that are electrically large or electrically small, respectively. A more detailed and rigorous analysis of this problem is presented in [20], but this simpler formulation appears to be adequate for the present problem. The total transmission cross section is expressed as

$$\langle \sigma_t \rangle \approx N_w \langle \sigma_{tw} \rangle \tag{11}$$

where N_w is the total number of windows in the cabin.

In subsequent steps, it is important to know not just the total power escaping from all windows, but specifically the power escaping from each window. It is assumed that the power escaping from each window is equal, independent of the location of the transmitter within the cabin. Of course, this cannot be exactly true, since one would intuitively expect that windows closer to the transmitter convey more power than those further away. However, this effect is believed to be strongly mitigated by the copious scattering that occurs within the cabin. This is most easily seen from a ray-optical viewpoint: any ray emerging from the transmitter is likely to have been reflected many times before escaping through a window; therefore, the window through which it escapes is essentially random. Evidence for this assumption is presented in [12], where it is found that the variation from window to window in relevant comparable scenarios is less than 5 dB at frequencies above VHF.

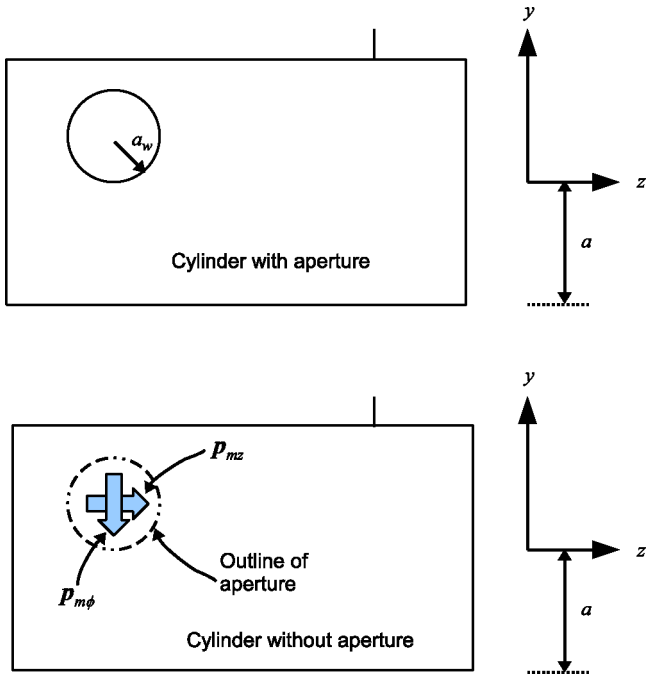

Fig. 1. Equivalent currents modeling radiation from a window.

B. Calculating Propagation Over the Fuselage

In the previous section, a method was described for estimating the power that escapes the cabin through windows. The problem of how to determine the power delivered to the victim antenna is now considered. The electric field emerging from any given window must "creep" along the surface of the fuselage in order to reach the victim antenna [21], [22]. The total electric field at the victim antenna is the sum of these contributions from all windows. Past work attempting to explain and quantify this mechanism by comparison of *in situ* measurements to measurements made under controlled conditions using simplified mock-ups have not yielded satisfactory results [4], [23]. In this section, an analytical approach is described that is simple, provides physical insight into the problem, and in combination with PBT seems to yield reasonable results, as shall be demonstrated in Section III.

Analysis begins with the problem of modeling the escape of fields through windows. It is well known that the problem of scattering by transmission through an aperture in a perfectly conducting surface can be modeled as the radiation of magnetic currents over the same area of the surface, but without the aperture [24]. In this procedure, the magnetic currents are determined by the enforcement of electromagnetic boundary conditions on the surface in the vicinity of the aperture. This is not possible in the present problem because expressions for the fields over the aperture are not available; instead, only the total power radiated by the aperture is known. To overcome this problem, the magnetic current distribution is modeled very simply as a pair of orthogonally polarized magnetic current moments, as shown in Fig. 1. Note the currents are located at the geometrical center of the aperture, tangent to the surface, and oriented parallel to and transverse to the axis of cylinder. Furthermore, it is assumed that each source is responsible for one-half of the power—an

assumption that is justified on the basis that one expects the escaping electric field to be randomly polarized as the result of many reflections within the cabin.

In order to use the model proposed earlier, it is necessary to determine the magnitude of current moments that give rise to the same amount of power known to be escaping from the given window. This can be determined as follows. Consider a current moment $\mathbf{p}_m = I_m L \hat{\mathbf{l}}$, where I_m is the magnetic current (having units of volts), L is length, and $\hat{\mathbf{l}}$ is a unit vector representing the polarization of the source. The far-field electric and magnetic fields arising from this source in free space are

$$\mathbf{E} = -\frac{jk}{4\pi}\,\mathbf{p}_m \times \hat{\mathbf{r}}\,\frac{e^{-jkr}}{r} \tag{12}$$

$$\mathbf{H} = +\frac{jk}{4\pi\eta}\,\mathbf{p}_m \times \hat{\mathbf{r}} \times \hat{\mathbf{r}}\,\frac{e^{-jkr}}{r} \tag{13}$$

where k is the free-space wavenumber $2\pi/\lambda$ and $\hat{\mathbf{r}}r$ is the vector pointing from the source point (center of the current moment) to the field point (point of measurement). The power P_p radiated by $\mathbf{p}_m$ in these conditions is determined by computing the Poynting (power density) vector associated with field described in (12) and (13), and then, integrating this over a sphere in the far field to determine the total power passing through the sphere. The answer is

$$P_p = \frac{k^2 |I_m|^2 L^2}{12\pi\eta}. \tag{14}$$

Since the total power radiated by $\mathbf{p}_m$ in the presence of the conducting screen must be the same, and since each current moment should account for half the total power radiated by the window, one finds

$$\mathbf{p}_{m\phi} = \hat{\phi}\sqrt{\frac{12\pi\eta P_p}{k^2}} \tag{15}$$

$$\mathbf{p}_{mz} = \hat{\mathbf{z}}\sqrt{\frac{12\pi\eta P_p}{k^2}} \tag{16}$$

for the two current moment sources modeling the window, where $P_p = P_T L_w/(2N_w)$ since the power escaping each window is assumed to be equal.

$$\mathbf{E}_p^r = -\frac{jk}{4\pi}\mathbf{p}_m \cdot \Bigg[2\Bigg(\hat{\mathbf{b}}'\hat{\mathbf{n}}\Bigg\{ \left(1 - \frac{j}{kt}\right) V(\xi) + T_0^2 \frac{j}{kt}\left[U(\xi) - V(\xi)\right] \Bigg\} + \hat{\mathbf{t}}'\hat{\mathbf{n}}\Bigg\{ T_0 \frac{j}{kt}\left[U(\xi) - V(\xi) \right] \Bigg\} \Bigg) \Bigg] \frac{e^{-jkt}}{t} \tag{17}$$

The electric field produced by a magnetic current moment $\mathbf{p}_m$ on the surface of a perfectly conducting cylinder, at some other point on the surface, is given by (17) [14], where the parameters are described as follows.

1) t is the distance from the source to the field point along the geodesic (shortest surface) path. Using the coordinate system implied in Fig. 1, $t = \sqrt{(a\Delta\phi)^2 + (\Delta z)^2}$ where a is the radius of the cylinder modeling the fuselage, $\Delta\phi$ is the angular separation between source and field points along ϕ, and Δz is the separation along z.
2) $\hat{\mathbf{n}}$ is the unit normal vector at the field point (i.e., the location of the victim antenna).
3) $\hat{\mathbf{t}}'$ is a unit vector tangent to the surface, pointing from the source point in the direction of the geodesic to the field point; see Fig. 2.
4) $\hat{\mathbf{b}}' = \hat{\mathbf{t}}' \times \hat{\mathbf{n}}'$, where $\hat{\mathbf{n}}'$ is the unit normal vector at the source point.
5) $T_0 = \cot\delta$, where δ is the angle, measured in the plane tangent to the source point, between the axis of the cylinder and $\hat{\mathbf{t}}'$.
6) $\xi = mt/\rho_g$ where $m = (k\rho_g/2)^{1/3}$ and $\rho_g = a/\sin^2\delta$.
7) $V(\xi)$ and $U(\xi)$ are the "hard surface" and "soft surface" Fock integrals, respectively, described in [14].

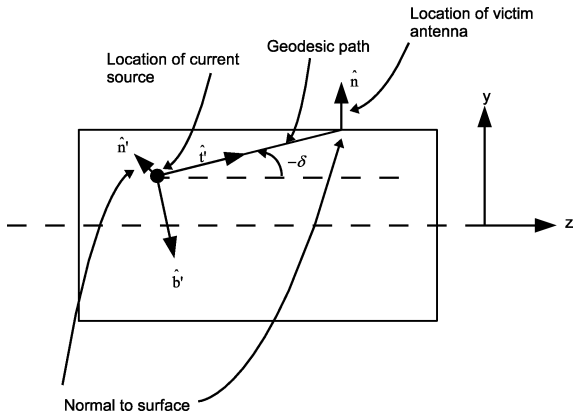

Fig. 2. Geometry for use of (17).

Note that (17) is written in compact dyadic notation; for example, "$\mathbf{p}_m \cdot \hat{\mathbf{b}}'\hat{\mathbf{n}}$" is interpreted as $(\mathbf{p}_m \cdot \hat{\mathbf{b}}')\hat{\mathbf{n}}$. Consequently, it is seen that $\mathbf{E}_p^r$ is completely $\hat{\mathbf{n}}$-polarized, as required by the relevant boundary conditions.

The electric field incident on the victim antenna $\mathbf{E}^r$ is the sum of the electric fields ($\mathbf{E}_p^r$'s) due to the $2N_w$ individual current moment sources, each calculated separately according to (17). The resulting power delivered to the antenna terminals under matched load conditions is [24]

$$P_R = \frac{1}{8R_A}\left|\mathbf{E}^r \cdot \mathbf{l}_e\right|^2 \tag{18}$$

where R_A is the radiation resistance (i.e., the real part of the antenna impedance) and $\mathbf{l}_e$ is the vector effective length of the victim antenna. For an ideal thin quarter-wave monopole, $R_A \approx 36\ \Omega$ and $\mathbf{l}_e = \hat{\mathbf{n}}\lambda/(2\pi)$, assuming the surface curvature is small compared to a wavelength. Although this is not necessarily an accurate model for any other antenna that might be used, a quarter-wave monopole serves as useful "worst case" scenario since it has maximum gain uniformly distributed along the horizon. The result for any other antenna can be calculated by applying the expected difference in gain with respect to that of a quarter-wave monopole.

Two important limitations of this method should be noted. First, it is assumed that the electric field associated with any

path longer than the shortest geodesic path (see Fig. 2) is either suppressed by blockage or is much weaker than the field associated with the shortest path. This will be justified by experiment in the next section. Second, the method is clearly limited to scenarios in which the shortest geodesic path from each window to the victim antenna is unobstructed, and that any other significant mechanism for power transfer from window to antenna is insignificant, e.g., reflection from winglets. As a result, the method as explained here is applicable mainly to victim antennas located on the dorsal region of the fuselage, and cannot necessarily be used for antennas located on the underside of the fuselage, or on wings or tail surfaces, without additional modifications to account for the new scattering geometry. However, these modifications are quite feasible [25]. Antennas located on the bottom half of the fuselage are known to experience significantly greater IPL, presumably since wings are likely to block some of the propagation paths [26].

Finally, it should be noted that this method is essentially a "high-frequency" technique and requires that the surface curvatures of the fuselage be small relative to a wavelength in order for the UTD creeping wave formulation to yield accurate results. A typical transport aircraft has $a > 2$ m, which corresponds to $ka > 4.9$ for frequencies greater than 118 MHz. This suggests (17) is applicable over most of the frequencies commonly used in commercial aviation, as previously demonstrated in [15]. Under no circumstances should the proposed method be considered to be valid at VHF frequencies or below, since in this regime, mechanisms such as coupling onto wires and propagation through door seams, which are neglected by the proposed method, become important.

C. Summary of the Method

The method for finding the IPL from any point (unspecified) in the cabin to a victim antenna located on the dorsal area of the fuselage is summarized as follows.

1) Compute L_w using (5). If the transmitting antenna is known to be located very close to a window, then radiation direct from the transmitting antenna through the window is important and $L_w = 0.5$ may be a better choice if the window is electrically large. (See further discussion of this in Section III-B.)
2) Determine $\mathbf{p}_{m\phi}$ and $\mathbf{p}_{mz}$ for each window using (15) and (16), respectively, with $P_p = L_w/(2N_w)$ (this can be interpreted as being power transmit through windows due to a 1-W emitter inside the cabin).
3) Determine the total electric field incident on the victim antenna by summing the contributions, determined using (17), of the $2N_w$ sources.
4) Determine P_R using (18). Assuming the 1-W normalization suggested in step 2, P_R can also be interpreted as the IPL.
5) Optionally, repeat steps 2–4, varying the phases of the source currents according to independent uniform random distributions, yielding the IPL distribution. From this, the mean IPL can be determined. The minimum IPL can be determined by forcing the electric fields to add coherently in step 3.

TABLE I
AIRCRAFT CONSIDERED IN THIS STUDY

Aircraft	Fuselage Radius a [m]	Fuselage Length L_f [m]	Number Seats N_s	Number Windows N_w
B727-200	1.88	41.5	134	94
B737-200	1.88	29.5	110	66
B747-400	2.42	68.8	416	194
B767-300	2.52	54.9	261	106
B777-200	3.11	62.9	305	128
A330-300	2.82	63.6	295	132

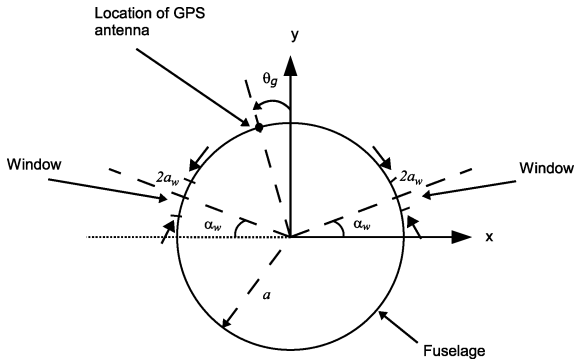

Fig. 3. Window geometry. In all cases simulated in this paper $\alpha_w = 20^\circ$ and $\theta_g = 0$ is assumed.

III. GPS IPL ESTIMATES

In this section, the method described in the previous section is applied to the calculation of IPL for the L1 frequency (1575.42 MHz) of GPS. The GPS antenna on an aircraft is located in the dorsal region and is therefore a good candidate for the method. Furthermore, measurement studies are available that can be used for comparison, as shall soon be discussed.

The aircraft considered are listed in Table I, along with the relevant dimensions. The manufacturer in each case is Boeing Corporation, except for the A330 that is manufactured by Airbus Corporation. Additional aircraft parameters are given in Fig. 3. For all aircraft, it is assumed that windows have effective radius $a_w = 14$ cm, which makes them electrically large [$ka_w > 1.29$, as per (9) and (10)] at frequencies greater than 440 MHz. The windows are assumed for the purposes of the present calculations to be evenly spaced along the length of the cabin, which is assumed to be $0.8L_f$, i.e., 80% of the length of the fuselage. The volume of the cabin for PBT purposes is then roughly estimated as

$$V = (0.8L_f)\left(\pi a^2\right)\frac{1}{2} \tag{19}$$

where the factor $1/2$ is an estimate of the cabin volume relative to the volume of the equivalent cylinder.

A. PBT Analysis

Results of the PBT analysis for these aircraft models are summarized in Table II. In this table, loss in people and seats

TABLE II
RESULTS OF PBT ANALYSIS AT 1575.42 MHZ (GPS L1)

Aircraft	Passenger Load	L_w [dB]	Total Q	Loss in People	Loss in Seats
B727-200	Full	−16.2	101	88.8%	8.9%
	50%	−13.7	181	79.8%	16.0%
	Empty	−6.7	893	0.0%	78.7%
B737-200	Full	−16.9	87	89.0%	2.1%
	50%	−14.3	158	80.0%	16.0%
	Empty	−7.3	798	0.0%	81.2%
B747-200	Full	−17.9	90	89.5%	8.9%
	50%	−15.4	162	80.9%	16.2%
	Empty	−8.2	851	0.0%	84.8%
B767-300	Full	−18.5	124	89.6%	9.0%
	50%	−16.0	225	81.2%	16.2%
	Empty	−8.7	1197	0.0%	86.5%
B777-200	Full	−18.4	185	89.6%	9.0%
	50%	−15.8	336	81.2%	16.2%
	Empty	−8.6	1780	0.0%	86.1%
A330-300	Full	−18.1	159	89.5%	9.0%
	50%	−15.5	288	81.0%	16.2%
	Empty	−8.3	1516	0.0%	85.3%

is indicated as the percent of total power transmitted that is dissipated in these media. In each case, the aircraft has been analyzed for passenger loads of 0% (empty, no passengers), 50%, and 100% (full; one passenger per seat assumed). An interesting finding is that all aircraft exhibit very similar results, and that it is instead the passenger load that is the dominant factor in determining the power transfer coefficient from transmitter to exterior (via windows) L_w. The effect of passenger load is especially evident in the "Loss in People" column. The factor L_w is seen to vary from about -7 dB to about -19 dB for 0% and 100% passenger load, respectively. It is also noted that the cabin Q is found to be in the range 89–1768. This appears to be consistent with reported measurements of a variety of aircraft that found cabin Q's to be in the range 10–1000, i.e., variable over about two orders of magnitude [27].

B. Single-Window IPL Analysis

Considered next is the part of the path loss associated with propagation from a window, along the surface of the fuselage, to the GPS antenna. Measurements of this mechanism for a Boeing 737 aircraft reported by Jafri *et al.* [7] provide a convenient source of data for comparison to predictions using the method. In these experiments, the IPL was measured for a linearly polarized transmit antenna located in a window, repeating the measurement for both vertical and horizontal transmit polarizations in each of the 33 windows on one side of the aircraft. Each of these measurements is modeled using the equivalent magnetic current moment, with the appropriate tangential orientation, as a source. Zero passenger load is assumed. It is also assumed that one-half of the total power radiated by the transmit

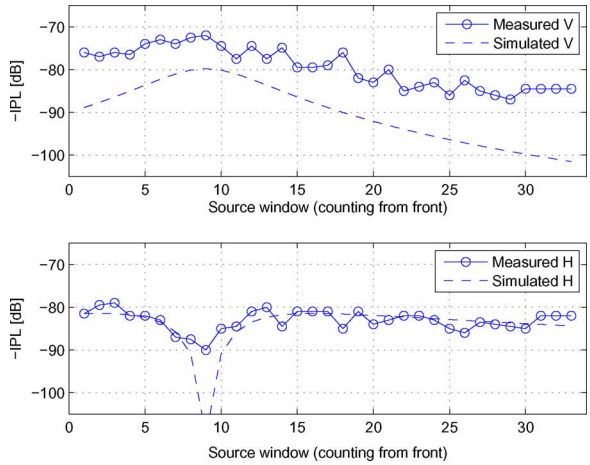

Fig. 4. Comparison of simulated and measured IPL data for vertical (V) and horizontal (H) polarizations of a transmit antenna placed in the indicated window. Note that IPL is shown in negative decibel, so that the vertical scale is proportional to signal strength.

antenna propagates into the aircraft and is lost. This is justified as follows: recall that the expected loss through windows (L_w) is about -7 dB (from Table II), thus the portion of the power that travels through the cabin and back out through other windows must be at least 7 dB less than the portion of the power that is radiated directly to the outside, and is spread across many windows such that the contributions arriving at the victim antenna from each window are unlikely to add coherently. Finally, it is assumed that the gain of the GPS antenna is uniformly 19 dB less than that of the reference resonant quarter-wave monopole for which results are initially computed. This is based on the understanding that the pattern of a patch antenna in the horizon plane is typically -20 dB below maximum (zenith) gain, which is about 6 dBi (e.g., see [28]). Thus, the appropriate correction for results computed assuming a quarter-wave monopole with 5 dBi horizon gain is -19 dB.

The results are shown in Fig. 4. Both measurements and simulation indicate that the dominant contribution for windows close to the GPS antenna (which is above window no. 9) is vertical polarization, whereas the dominant contribution is horizontal polarization for windows further away. Note that the agreement for the horizontal polarization is excellent, although given the crude nature of the GPS antenna modeling discussed earlier, this is possibly serendipitous. Nevertheless, the agreement in form including the prediction of a null associated with window no. 9 (which is directly under the GPS antenna) is very encouraging. The results for the horizontal polarization also exhibit the expected form, but with IPL 5–8 dB less than measurements for the region around window no. 9. For both measured and predicted results, the IPL decreases steadily with increasing distance from window no. 9, and the difference between measurements and prediction grows. These findings are consistent with previous analysis and measurements by Devereux *et al.* [21], who also demonstrated a similar trend in "per-window" IPL.

All aspects of this result are quite satisfactory except for the significant difference between measurement and simulation for vertical polarization when the source is in a window close

TABLE III
RESULTS OF SIMULATION ("SIM.") COMPARED TO RESULTS OF VARIOUS MEASUREMENT CAMPAIGNS ("MEAS")

Aircraft	Pasngr Load	Sim. Min. [dB]	Mean [dB]	Meas. Min. [dB]	Ref.
B727-200	Full	75	96		
	50%	73	94		
	Empty	66	87	71	[29], [10]
B737-200	Full	76	96		
	50%	73	93		
	Empty	66	86	64	[2]
B747-200	Full	79	103		
	50%	76	101		
	Empty	69	93	65	[2]
B767-300	Full	81	103		
	50%	79	101		
	Empty	72	93	91	[30]
B777-200	Full	84	106		
	50%	81	103		
	Empty	74	96	66	[30]
A330-300	Full	82	105		
	50%	79	102		
	Empty	72	95	76	[31]

to the GPS antenna. A possible explanation for this is that, in the measurements, much of the power that is transmitted directly into the aircraft emerges from the windows directly across the cabin from the window containing the source, and from there is able to contribute significantly to the result. One would expect this mechanism to be subdued for a horizontally polarized source, as reflections from the floor and ceiling would be out of phase and would therefore tend to cancel the fields that travel directly from window to window through the cabin. If this is so, one need not be concerned about this in IPL calculations for transmitters completely inside the cabin, since in that case, one expects closer-to-equal power flow from each window.

C. IPL Statistics

The full method described in Section II-C is now applied to determine IPL statistics for a source completely inside the cabin to the GPS antenna. Results are summarized in Table III. Note that both minimum IPL and mean IPL are computed. The mean IPL was determined using the method suggested in step 5 of the procedure in Section II-C. The minimum IPL was determined by choosing component electric field phases that added coherently to produce the maximum possible field incident on the antenna.

Fig. 5 is provided for ease in comparison. Note that the comparison is shown for two cases; in one case assuming in the simulation that the aircraft was empty during the stated measurements, and in the second case assuming 50% passenger load for simulation. The actual situation in reported measurements is typically not clear: whereas the measurements do not

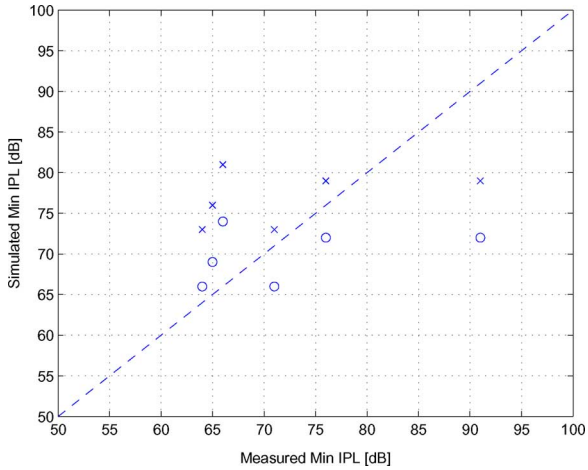

Fig. 5. Comparison of simulated and measured minimum IPL data from Table III. Circles ("○") correspond to simulations assuming empty conditions, where as the "×" correspond to simulations assuming 50% passenger load. The dashed line corresponds to perfect agreement.

involve passengers, in many cases, they seem to have involved significant numbers of workers in the cabin, or may have involved open doors or other conditions that would produce the same effect. This may account for the large variance in the measured results compared to the relatively small variance observed in the simulated results. Agreement within an order of magnitude seems to exist between simulation and measurement in most cases, although clearly with high variance and some outliers.

Two interesting observations from the simulated results are as follows: 1) regardless of the aircraft considered, the effect of increasing passenger load from 0% to 50% and then 50% to 100% is an increase of about 7 and 3 dB in IPL, respectively. Of course, this is could have been anticipated from the PBT results. 2) The variation from aircraft to aircraft is within an order of magnitude, at least in simulation. As implied before, the larger variation observed in measurements may be due to differences in measurement procedures used for each aircraft.

Finally, it is noted that specifically for the B737 aircraft, Table III indicates that simulation appears to be estimating IPL which is greater than measurement by between 2 and 9 dB. This may be consistent with the finding shown in Fig. 4; specifically, the contribution from the dominant vertical polarization of the source antenna is being underestimated by the proposed technique. However, examination of the results for other aircraft presented in Fig. 5 reveals that similar offsets are consistently not seen for all aircraft, and thus, the source of the discrepancy seen in the vertical source polarization results shown in Fig. 4 remains an open question.

IV. FREQUENCY DEPENDENCE OF IPL

The frequency dependence of IPL for the B737, which is the same aircraft considered in Section III-B and one of the aircraft considered in the previous section, is now considered. Table IV shows the frequencies considered and the results.

TABLE IV
PREDICTED MINIMUM IPL FOR A DORSAL-MOUNTED RESONANT QUARTER-WAVE MONOPOLE ON A B737 AIRCRAFT

			0% load		100% load		
f	ka	ka_w	L_w	IPL	L_w	IPL	System
118 MHz	4.6	0.3	−63.4 dB	71 dB	−73.8 dB	81 dB	VOR/VHF Voice
330 MHz	13.0	1.0	−45.5 dB	65 dB	−55.4 dB	75 dB	Glide Slope
962 MHz	37.9	2.8	−7.3 dB	40 dB	−16.9 dB	50 dB	DME
1227 MHz	48.3	3.6	−7.3 dB	44 dB	−16.9 dB	53 dB	GPS L2
1575 MHz	62.0	4.6	−7.3 dB	47 dB	−16.9 dB	57 dB	GPS L1
5060 MHz	199.2	14.8	−7.3 dB	66 dB	−16.9 dB	76 dB	MLS

Frequencies were selected to correspond to receive frequencies of potentially vulnerable flight systems. To provide a uniform comparison with changing frequency, the antenna was assumed to be a quarter-wave monopole that is resonant at that frequency, at the same location as the existing GPS antenna. (Obviously, the actual IPL will be significantly different because each system may use a different antenna located at a different position on the aircraft.) For each frequency, the electrical radius of the fuselage ka and electrical radius of a window ka_w are indicated. Note that ka is relatively large even at frequencies as low as 118 MHz, providing some confidence that the UTD approach described in Section II-B is reasonable. Also note that ka_w is in the "electrically small" regime for 118 and 330 MHz, which has the effect of choking off power transmission through windows (quantified as L_w) and thereby greatly increasing IPL. However (as previously noted), it is expected that the mechanisms of coupling onto wiring and propagation through door seams become important in this frequency regime; thus, the prediction of reduced IPL may not be valid in this case. Above the window's "cutoff frequency" in the UHF range, L_w is effectively constant with frequency because the frequency dependencies of Q_2 and Q_3 are identical [see (6) and (7)] to the extent that the absorption and transmission cross sections are assumed to be frequency independent. Despite this, IPL rolls off at high frequencies due to increased loss in the creeping wave propagation from window to victim antenna. This results in a worst-case IPL that occurs (with respect to the frequencies appearing in the table) at 962 MHz. Finally, it is noted that, independent of the frequency, the difference between 0% and 100% passenger load is consistently a difference of about 10 dB in IPL.

V. CONCLUSION

This paper presents a technique, summarized in Section II-C, for predicting the IPL for an important class of aircraft interior-to-exterior propagation problems. The technique yields estimates with minimal computational burden and does not require detailed information about cabin configuration. It was demonstrated in Section III-B (using the GPS L1 system on a Boeing 737 as a representative example) that the UTD-based method employed by our technique yields reasonable agreement with the results of published measurements of the window-to-antenna coupling mechanism, although perhaps underestimating the contribution of the dominant vertical polarization for the shortest path lengths. In Section III-C, it was demonstrated that the complete technique nevertheless yields values for the cabin-to-antenna IPL that are within an order of magnitude of published measurements for a number of large transport aircraft in most cases.

The data provided by the technique in the investigation in Section III reveal that all large transport aircraft exhibit very similar results, and that it is instead the passenger load that is the dominant factor in determining the power transfer coefficient from transmitter to exterior. It is also found that, regardless of the aircraft considered, the effect of increasing passenger load from 0% to 50% and then 50% to 100% is an increase of about 7 and 3 dB in IPL, respectively. The variation in simulation results from aircraft to aircraft is within an order of magnitude for the aircraft considered in this study. The larger variation observed in reported measurements may be due to differences in measurement procedures used for each aircraft.

The key advantage of this technique over full-wave modeling is computational burden, which is very low and roughly independent of frequency. In Section, the method was employed to compute IPL for frequencies from 118 MHz to 5 GHz. It was found that the worst-case IPL occurs at about 1 GHz, with IPL decreasing at lower frequencies because the windows become electrically small and "choke off" leakage to the outside, and IPL decreasing at higher frequencies because of increasing path loss for the "creeping wave" propagation from window to antenna. Finally, it is noted that, independent of the frequency, the difference between 0% and 100% passenger load is a difference of about 10 dB in IPL.

Further development and evaluation is warranted to more clearly determine the fidelity with which the proposed technique can predict IPL. Performance of the method proposed here should first be validated in measurements on simplified test models that satisfy as closely as possible the assumptions made in developing the model. A method for accounting for radiation direct from the transmitter preferentially to nearby windows, not included here, should be considered. Subsequent efforts require supporting measurements on actual aircraft at a variety of frequencies in order to truly facilitate "apples to apples" comparison across aircraft types and frequencies, and also to obtain specific diagnostic measurements needed to test hypotheses about relevant scattering mechanisms, e.g., testing IPL on a window-by-window basis, varying passenger load levels, and so on. Finally, the technique described here can be

straightforwardly extended to allow calculations for antennas located *anywhere* on the aircraft (not just along the dorsal area), using additional UTD diffraction terms to account for the influence of wings, engines, and other structures.

ACKNOWLEDGMENT

This paper was significantly improved through the efforts of the reviewers, who identified some relevant references and pointed out some limitations of the proposed method that had been overlooked.

REFERENCES

[1] *2001 Federal Radionavigation Systems*, DOT-VNTSC-RSPA-0103.1/DOD-4650.5, U.S. Depts. Def. and Transp., Washington, DC, 2001.

[2] RTCA SC-202, "Guidance on allowing transmitting portable electronic devices (T-PEDs) on aircraft," RTCA, Inc., Washington, DC, DO-294B, Dec. 2006 (change 1 released Dec. 2007).

[3] RTCA SC-202, "Aircraft design and certification for portable electronic devices (PED) tolerance," RTCA, Inc., Washington, DC, DO-307, Oct. 2007.

[4] G. Fuller, "Comparison of cylindrical mock-up path loss data to operational aircraft data. Determining path loss variations with distance and radius at VHF, L Band, and GPS/Satcom," in *Proc. 19th Digit. Avionics Syst. Conf.*, Philadelphia, PA, Oct. 7–13, 2000, vol. 1, pp. 3.B.4-1–3.B.4-8.

[5] S. Potsch, A. Enders, M. Grossmann, R. Kebel, and H.-W. Kruger, "Reliable transfer function measurements of PED excitations in aircrafts," in *Proc. IEEE Int. Symp. Electromagn. Compat.*, Aug. 2003, vol. 2, pp. 537–542.

[6] M. J. Jafri, J. J. Ely, and L. Vahala, "Graphical analysis of B-737 airplane pathloss data for GPS and evaluation of coupling mitigation techniques," in *Proc. 2004 IEEE Int. Symp. Electromagn. Compat.*, Aug. 2004, vol. 3, pp. 832–837.

[7] M. Jafri, J. Ely, and L. Vahala, "Comparative analysis of interference path loss coupling patterns on B-737 vs. B-757 airplanes," in *Proc. 24th Digit. Avionics Syst. Conf. (DASC 2005)*, Oct./Nov., vol. 1, pp. 6.B.5-1–6.B.5-10.

[8] K. Horton, M. Huffman, B. Eppic, and H. White, "757 path loss measurements," NASA, Washington, DC, Tech. Rep. CR-2005-213762, Jun. 2005.

[9] T. X. Nguyen, S. V. Koppen, J. J. Ely, G. N. Szatkowsky, J. J. Mielnik, and M. T. P. Salud, "Small aircraft RF interference path loss," in *Proc. IEEE Int. Symp. Electromagn. Compat. (EMC 2007)*, Jul., pp. 1–6.

[10] J. J. Ely, T. X. Nguyen, S. V. Koppen, and M. T. Salud, "Electromagnetic interference assessment of CDMA and GSM wireless phones to aircraft navigation radios," in *Proc. 21st Digit. Avionics Syst. Conf.*, Irvine, CA, Oct. 27–31, 2002, vol. 2, pp. 13E4-1–13E4-13.

[11] C. Waldschmidt, J. V. Hagen, H.-L. Blocher, K. Beilenhoff, J. Wenger, and W. Wiesbeck, "Wave propagation modelling in confined spaces," in *Proc. IEEE 56th Veh. Technol. Conf.* (VTC-2002 Fall), Sep., vol. 2, pp. 1056–1059.

[12] R. W. Devereux, G. L. Fuller, and R. Schillinger, "Further analysis of the CV-580 and B-727 aircraft RF coupling experiment data," in *Proc. 16th Digit. Avionics Syst. Conf.*, Oct., 1997, vol. 1, pp. 4.1-1–4.1-8.

[13] D. A. Hill, M. T. Ma, A. R. Ondrejka, B. F. Riddle, M. L. Crawford, and R. T. Johnk, "Aperture excitation of electrically large, lossy cavities," *IEEE Trans. Electromagn. Compat.*, vol. 36, no. 3, pp. 169–178, Aug. 1994.

[14] P. H. Pathak and N. Wang, "Ray analysis of mutual coupling between antennas on a convex surface," *IEEE Trans. Antennas Propag.*, vol. AP-29, no. 6, pp. 911–22, Nov. 1981.

[15] E. M. Koper, W. D. Wood, and S. W. Schneider, "Aircraft antenna coupling minimization using genetic algorithms and approximations," *IEEE Trans. Aerosp. Electron. Syst.*, vol. 40, no. 2, pp. 742–751, Apr. 2004.

[16] Y. Yamaguchi, T. Abe, and T. Sekiguchi, "Radio propagation characteristics in underground streets crowded with pedestrians," *IEEE Trans. Electromagn. Compat.*, vol. 30, no. 2, pp. 130–136, May 1988.

[17] M. Ghaddar, L. Talbi, and T. A. Denidni, "Human body modelling for prediction of effects of people on indoor propagation channel," *Electron. Lett.*, vol. 40, no. 25, pp. 1592–1594, Dec. 2004.

[18] S. W. Ellingson, Virginia Polytech. Inst. State Univ., private communication, 2002.

[19] T. X. Nguyen, "RF loading effects of aircraft seats in an electromagnetic reverberating environment," NASA Langley Research Center, Hampton, VA, NASA TM-2000-210626, Dec. 2000.

[20] X. Cao, K. M. Luk, C. Liang, and J. Gao, "Analysis of aperture coupling of electromagnetic energy in cylindrical wall," *IEEE Antennas Wireless Propag. Lett.*, vol. 3, no. 1, pp. 79–82, 2004.

[21] R. W. Devereux, B. Archambeault, and G. L. Fuller, "Assessment of aircraft internal EMI using electromagnetic analytical modeling codes," in *Proc. 17th Digit. Avionics Syst. Conf.* 31 Oct.–7 Nov., 1998, vol. 1, pp. D41/1–D41/8.

[22] R. W. Devereux and G. L. Fuller, "Coupling and vulnerability of CNI systems to an onboard RF source," in *Proc. 17th Digit. Avionics Syst. Conf.* 31 Oct.–7 Nov., 1998, vol. 1, pp. D46/1–D46/8.

[23] G. Fuller, "Path loss measurements on cylindrical sections. Determining path loss variations with distance and radius at VHF, L Band, and GPS/Satcom," in *Proc. 19th Digit. Avionics Syst. Conf.*, Philadelphia, PA, Oct. 2000, vol. 1, pp. 3B3/1–3B3/7.

[24] W. A. Stutzman and G. A. Thiele, *Antenna Theory and Design*, 2nd ed. New York: Wiley, 1998.

[25] R. J. Marhefka and W. D. Burnside, "Antennas on complex platforms," *Proc. IEEE*, vol. 80, no. 1, pp. 204–208, Jan. 1992.

[26] G. Fuller and K. Horton, "The relationship of commercial aircraft fuselage size on RF coupling/path loss from RF sources to receiver-based navigation and communication avionics systems," in *Proc. 18th Digit. Avionics Syst. Conf.*, Oct., 1999, vol. 2, pp. 10.B.4-1–10.B.4-4

[27] G. J. Freyer, M. O. Hatfield, and M. B. Slocum, "Characterization of the electromagnetic environment in aircraft cavities excited by internal and external sources," in *Proc. 15th Digit. Avionics Syst. Conf.*, Oct., 1996, pp. 327–332.

[28] C. A. Balanis, *Antenna Theory: Analysis and Design*, 3rd ed. New York: Wiley, 2005.

[29] RTCA SC-156, "Potential interference to aircraft electronic equipment from devices carried aboard," RTCA, Inc. Washington, DC, DO-199, Sep. 16, 1988.

[30] Delta Airlines, "Delta/NASA cooperative agreement NCC-1-381 deliverable reports," Delta Airlines, Atlanta, GA, Delta Eng. Rep. 10-76052-20, Dec. 7, 2000.

[31] EUROCAE Working Group 58, "Report on electromagnetic compatibility between passenger carried electronic devices and aircraft systems," Document ED-118, Nov. 2003 (information obtained via [2]).

Kathy Wei Hurst received the B.S. and M.S. degrees in electrical engineering from Virginia Polytechnic Institute and State University, Blacksburg, in 2006 and 2007, respectively.

She is currently with the United States Patent and Trademark Office, Alexandria, VA, where she is engaged in the area of wireless communication.

Steven W. Ellingson (S'87–M'90–SM'03) received the B.S. degree in electrical and computer engineering from Clarkson University, Potsdam, NY, in 1987, and the M.S. and Ph.D. degrees in electrical engineering from The Ohio State University, Columbus, in 1989 and 2000, respectively.

From 1989 to 1993, he was with the U.S. Army. From 1993 to 1995, he was a Senior Consultant with Booz-Allen and Hamilton, McLean, VA. From 1995 to 1997, he was a Senior Systems Engineer with Raytheon E-Systems, Falls Church, VA. From 1997 to 2003, he was a Research Scientist with The Ohio State University ElectroScience Laboratory. Since 2003, he has been an Assistant Professor in the Bradley Department of Electrical and Computer Engineering, Virginia Polytechnic Institute and State University, Blacksburg. His current research interests include antennas and propagation, applied signal processing, and instrumentation.